International Journal of Industrial Electronics, Control and Optimization © 2020 IECO
Vol. 3, No. 1, pp. 11-18, jan(2020)

A Portable Power Generation System: Axial Flux PM Generator Design

Reza Yazdanpanah†

Department of Electrical Engineering, University of Larestan, Lar, Iran

ABSTRACT

Design methodology of a compact size charging system for emergency uses is investigated in this paper. The system consists of a gearing unit, a generator, a charger, and some battery cells. The system's electrical model has been introduced and a 3-phase axial flux surface mounted PM generator with a concentrated winding is picked as a generation unit. The basic equations needed for the generator design are presented as well as the general considerations and constraints for the designs. After validating the design equations using Finite Element Analysis, sizing equations are used to design different machines. The resulted designs are compared based on main characteristics including output power, power delivered to the battery, and generator efficiency. Finally, the performance of the valid designs in the system model is analyzed over a wide speed range. The proposed methodology could be used to design portable power generation units for such applications as rescuing, power system outage, camping, and so on.

Article Info

Keywords:
Axial flux, Design, Finite Element, Optimization,
Permanent Magnet Synchronous Generator, Portable Power Generation

Article History:
Received 2018-11-30
Accepted 2019-05-26

I. INTRODUCTION

Generators are an important part of human-driven portable power generation systems. These generation units can be applied to charge batteries and supply temporary loads for different applications such as rescuing, power system outage, camping, etc. Hence, high power density, efficiency, and compact size are three main designing criteria of these systems.

The portable power generation systems consist of (i) a gear unit to transform the human arm energy to the desired rotation of the generator, (ii) a generator, (iii) a battery charger unit, and (iv) a battery. Compared to the other types of generators, axial flux permanent magnet (AFPM) generators are more attractive, especially in low power applications due to their higher power density and efficiency [1-3]. In addition, their benefit from the cost, mass and volume viewpoints is that they do not need a power supply for feeding and controlling the excitation. In addition, gear units and generators can be combined to further minimize the total mass and space of the system [4]. For variable-speed direct-driven applications such as wind turbines, automotive applications, or human power generation, different types of PM generators followed by a converter as a power flow controller are the known combinations [5-8].

For the design optimization and parametric analysis, analytical equations of electromagnetic systems are the general and well-known efficient, fast and reliable methods for the primary design of electric machines [9-11]. In this paper, AFPM is picked as a generator of the system. The basic equations needed for the AFPM generator design are presented and the general design considerations and limitations are introduced and considered. Finite element analysis (FEA) is a powerful tool [12,13] utilized for validating the analytical design procedure.

This paper is organized as follows. Section II presents the system design considerations including an electrical model of the system, converter, and AFPM generator design method as well as equations and constraints. Then, the design equations are validated by a numerical simulation of the system in Section III and Section IV evaluates the performance of the portable power generation system over the operation range. Conclusions are drawn in Section V.

†Corresponding Author: ryazdanpanah@lar.ac.ir
Tel: +98-7152253105, Fax: +98-7152251892, University of Larestan
Department of Electrical Engineering, University of Larestan, Lar, Iran

II. DESIGN CONSIDERATIONS

The architecture of the portable power generation system is shown in Fig. 1. The system consists of a generator, power flow control unit, and storage. It is clear that a lighter device is preferred, but this parameter is affected by the physical and electromagnetic properties of the used material, especially the iron parts of the system. The main iron parts of the system are the stator and the rotor of the generator. Materials with higher saturation level reduce the use of iron which results in lower overall volume and mass of the system. Also, using PMs with a higher energy density like rear earth PMs will directly reduce the size of the generator. So, a design approach is presented below to find the optimum design for a portable power generation system.

A. Electrical model

A portable power generation system consists of four basic parts each of which can be represented by an electrical circuit. The system is shown in Fig. 1a. The power electronic interface rectifies and controls the 3-phase AC power from the output of the generator to be delivered to the battery storage. To have a reliable charging process, two types of converters can be utilized: 1) uncontrolled rectification of the output power of the generator, 2) controlled rectification using a chopper in series with the previous rectification stage.

The DC equivalent model of the system is shown in Fig. 1b. The model has a three-phase generator connected to a diode rectifier that is modeled by its open-circuit DC voltage E_{dc}, equivalent resistance R_{dc}, and the equivalent overlap resistance $R_{overlap}$ due to commutating inductance [14,15].

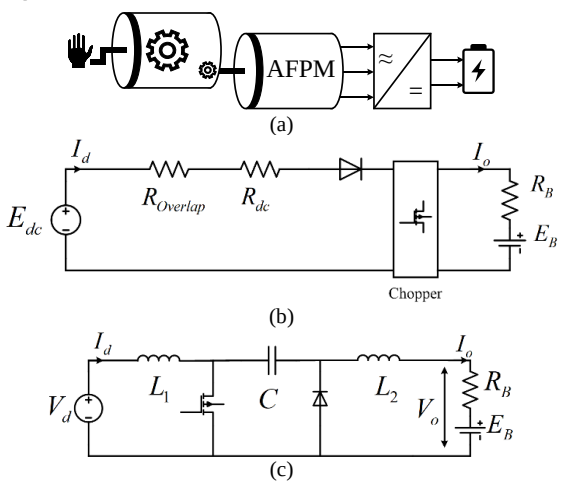

Fig. 1. A portable power generation system: a) schematic b) the equivalent DC model, c) a chopper (Cuk-converter) circuit

For a three-phase bridge rectifier, we have [15]:

$$R_{dc} = 2R_s \tag{1}$$

$$R_{overlap} = \frac{3}{\pi}\omega_e L_s \tag{2}$$

$$E_{dc} = \frac{3\sqrt{6}}{\pi}E \tag{3}$$

So, the rectifier output is:

$$V_d = E_{dc} - I_d(R_{dc} + R_{overlap}) - V_{diode} \tag{4}$$

where $\omega_e, E, R_s, L_s, I_d$, and V_d are the generator frequency, phase back-EMF, resistance, inductance, and output DC current and voltage of the rectifier, respectively.

When a diode bridge is supplied by a source with inductance and the DC side is represented by a current source, the current commutation will not be instantaneous and the maximum ideal value of the commutation angle u should be less than $\pi/3$ [6], [16].

B. Chopper design and battery modeling

A Cuk converter (Fig. 1c) is designed and implemented as a DC/DC converter due to its buck-boost capability and continuous input and output currents to regulate the charging profile independent of back-EMF of the generator due to different speeds of the rotation by the human arm [15].

The battery is modeled by its equivalent DC resistance R_B in series with a voltage source E_B. So, the delivered power to the battery P_{del} is:

$$P_{del} = I_o.E_B \tag{5}$$

By the circuit equations and assuming lossless operation of the converter, the following relation is obtained [16]:

$$\frac{V_o}{V_d} = \frac{I_d}{I_o} = \frac{D}{1-D} \tag{6}$$

where, D is the duty ratio defined as the ratio of switch on-time to switching period. And:

$$I_o = \frac{V_o - E_b}{R_b} \tag{7}$$

So, to operate the converter in the continuous input and output currents mode:

$$\begin{cases} I_{L1} - \Delta I_{L1} \geq 0 \\ I_{L2} - \Delta I_{L2} \geq 0 \end{cases} \tag{8}$$

By substituting parameters in (7), we have:

$$\begin{cases} \left(\frac{V_o - E_b}{R_b}\right)\left(\frac{D}{1-D}\right) - \frac{V_d D}{2L_1 f} \geq 0 \\ \frac{V_o - E_b}{R_b} - \frac{V_d D}{2L_2 f} \geq 0 \end{cases} \tag{9}$$

So, L_1 and L_2 can be defined with design criteria. For certain allowable ripple of the capacitor ΔV_C, its value can also be calculated with:

$$C \approx \frac{\left(\frac{V_o - E_b}{R_b}\right)D}{f\Delta V_C} \tag{10}$$

C. AFPM Design

The following assumptions are taken into account in the generator design [7]:

- the fundamental component of the magnetic flux density distribution in the air-gap is only considered
- magnetic flux crosses the air-gap perpendicularly

To reduce manufacturing costs and the winding losses, concentrated windings for stator are developed with shorter end windings, reduced copper losses, higher torque density, potentially higher efficiency, and easiness to manufacture [17-19].

Fig. 2 shows a cross-section of a concentrated windings machine. The peak value of the fundamental space harmonic of the magnetic flux density in the air-gap can be calculated by Ampere's circuital law, the magnetic flux continuity and the Fourier analysis as below [7]:

$$\hat{B}_g = \frac{l_m}{\mu_{rm} g_{eff}} B_{rm} \frac{4}{\pi} \sin\left(\frac{\pi b_p(r)}{2\tau_p(r)}\right) \tag{11}$$

where B_{rm} , μ_{rm}, l_m and g_{eff} are the residual flux density, relative recoil permeability and thickness of the PMs, and the effective air-gap length, respectively. In addition, $\tau_p(r)$ is the pole pitch and $b_p(r)$ is the width of the PMs at radius r . For a non-sinusoidal magnetic flux density waveform, the magnetic flux produced by the PMs per pole is [9]:

$$\Phi_f = \int_{r_i}^{r_o} \left(\frac{2}{\pi} \hat{B}_g \frac{\pi}{p} r\right) dr \tag{12}$$

For rectangular shape PMs with the width of b_p , Eq. (12) results in:

$$\Phi_f = \frac{l_m}{\mu_{rm} g_{eff}} B_{rm} \frac{8}{\pi p} \int_{r_i}^{r_o} \sin\left(\frac{p.b_p}{2r}\right) dr \tag{13}$$

where p is the number of pole-pairs and r_i, r_o are the inner and outer radii of the poles, respectively.

The no-load voltage induced in each phase can be calculated as below [9]:

$$E = \frac{1}{\sqrt{2}} k_w N_s \omega \left(r_o^2 - r_i^2\right) \hat{B}_g \tag{14}$$

where k_w is the distribution factor for the fundamental space harmonic, ω is the mechanical angular speed, and N_s is the number of turns per phase.

The average length of a turn and the average length of the inner and outer end turns can be calculated as follows [20]:

$$l_m = 2\left(r_o - r_i + 0.5 b_s\right) + \frac{2\pi(r_o + r_i)}{s} \tag{15}$$

$$l_{m,end\,turn} = \frac{\pi(r_o + r_i)}{s} + 0.5 b_s \tag{16}$$

where s is the number of slots.

A double-layer winding has shorter end-windings, lower MMF harmonic contents, eddy current losses in the PMs, and leakage inductance [21].

For the double-layer winding, the cross-section area of a conductor is:

$$a_{cu} = \frac{b_s h_s k_{fill}}{2N_c} \tag{17}$$

where N_c is the coil number of turns, k_{fill} is the slot fill-factor, and b_s, h_s are the width and depth of the slot, as shown in Fig. 2. So, the coil and phase resistances will be calculated. For a double-layer concentrated winding, the specific leakage, the end connection, and differential leakage fluxes are calculated by Eq. (19)-(20), respectively [9].

$$\lambda_{1s} = \left(\frac{h_s - h_{12}}{3b_s} + \frac{h_{12}}{b_s}\right) \frac{3(\omega_c / \tau_p) + 1}{4} \tag{18}$$

$$\lambda_{1e} = 0.34q\left(1 - \frac{2}{\pi} \frac{\omega_c}{l_{m,end\,turn}}\right) \tag{19}$$

$$\lambda_{1d} = \frac{mq\tau_p k_w^2}{\pi^2 g_{eff} k_{sat}} \left[\frac{\pi^2(10q^2+2)}{27}\left(\sin\left(\frac{30}{q}\right)\right)^2 - 1\right] + \frac{5g'/b_s}{5 + 4g'/b_s} \tag{20}$$

where g_{eff} and g' are defined in [9] and ω_c , q , m , and k_{sat} are the coil pitch, the number of slots per-pole per-phase, the number of phases, and the saturation factor of the magnetic circuit, respectively.

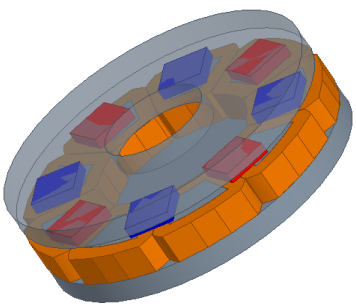

(a)

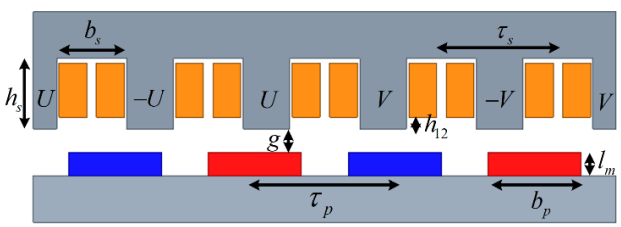

(b)

Fig. 2. An axial flux single rotor PM generator with concentrated winding: a) AFPM structure, b) cross-section and geometrical parameters

The armature leakage reactance is:

$$X_1 = 4\pi f \mu_0 \frac{L_i N_s^2}{pq} \left(\lambda_{1s} + \frac{2l_{m,end\,turn}}{L_i} \lambda_{1e} + \lambda_{1d}\right) \tag{21}$$

where L_i is the effective length of the stack.

The armature reaction reactance assuming $\mu_{rm}=1$ and surface configuration of PMs is [9]:

$$X_a = 2m\mu_0 f\left(\frac{N_s k_w}{p}\right)^2\left(\frac{r_o^2 - r_i^2}{g_{eff}}\right) \quad (22)$$

So, the synchronous reactance of a machine is calculated as below:

$$X_s = X_1 + X_a \quad (23)$$

Electric and magnetic constraints of an electric machine can be considered by the peak line current density in the average radius [9]:

$$A_m = \frac{2\sqrt{2}mI_a N_s}{\pi(r_o + r_i)} \quad (24)$$

and the magnetic flux density in the narrowest stator tooth part [19]:

$$B_{t,\max} = \frac{\hat{B}_g.\tau_{s,\min}}{b_{t,\min}} \quad (25)$$

where I_a is the armature current, $\tau_{s,\min}$ is the minimum slot pitch, and $b_{t,\min}$ is the narrowest tooth width at the inner radius.

For a generator with an output power P_g, by assuming the core and PM losses k_{loss} times of the output power, the electromagnetic power can be calculated as [21,22]:

$$P_{elm} = (1+k_{loss})P_g + \Delta P_w \quad (26)$$

where ΔP_w is the stator winding losses. Now, the efficiency of the generator is:

$$\eta = \frac{P_g}{P_{elm}} \quad (27)$$

The cogging-torque frequency is given by the smallest common multiplier of the number of poles and slots [6]. For a slot to pole ratio of 9/8, 15/14, 12/10, 12/14 and 18/16, very good results are obtained [6].

So, the preliminary design specifications of the AFPM generator are as following:

- double-layer concentrated winding with 9/8 slot to pole ratio
- minimum possible slot depth and so axial length
- maximum peak line current density in the average radius $A_{m,\max}$
- maximum magnetic flux density in the narrowest part of the stator tooth $B_{\max}$

The generator design variables to meet the minimum requirements are PM width (b_p) and thickness (l_m), slot width to pitch ratio (b_s/τ_s), h_s and h_{12}, and phase number of turns (N_s).

Table I shows the main design parameters in which some parameters are held constant and the constraints are applied for minimum delivered power to the battery and the generator efficiency.

By taking the constant parameters and the design constraints into account, and sweeping the design variables, including geometric and electromagnetic parameters, the valid designs are resulted as reported in Table II. Fig. 3 compares the main characteristics of valid designs.

To design higher power generators, some constant parameters and design constraints should be changed so that the design process could be converged to valid designs. These parameters and constraints are geometrical parameters (outer radius, maximum slot height) and PM parameter (width and thickness).

III. FEA VALIDATION OF THE DESIGNS

This section validates the analytical design equations. The system is implemented in the FEA software package. Also, a MATLAB code is generated to calculate the field variables using the analytical deign equations as described in Section II.

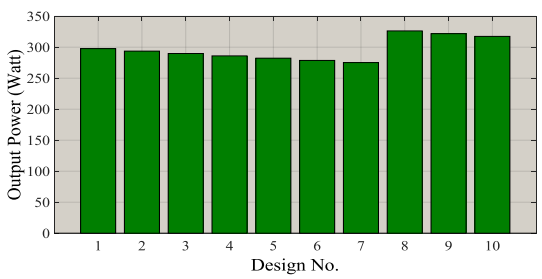

Fig. 3(a)

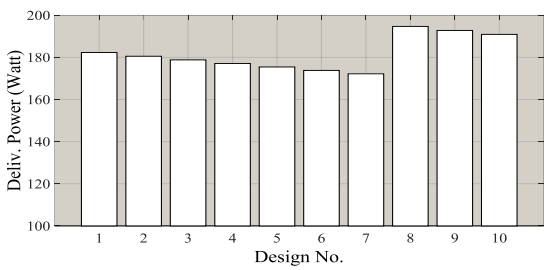

Fig. 3(b)

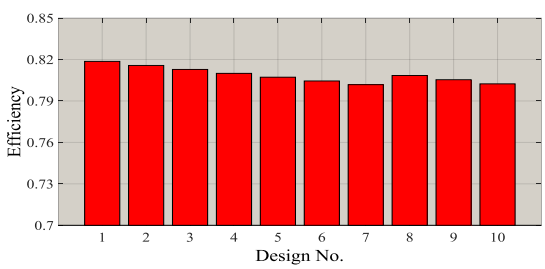

(c)

Fig. 3. The comparison of the main characteristics of the valid designs: a) output power, b) power delivered to the battery, c) generator efficiency

Fig. 4 shows the magnetic flux density distribution in different parts of the 1st design generator as well as the back-EMF. The duty ratio of the controlled converter is set to 0.5.

The main characteristics and output parameters of the generator and the portable power generation system are compared in Table III that shows the close results of analytical and numerical solutions. Discrepancies in analytical and numerical results of Table III are mainly due to simplifying a complex structure to a 2D linear model, neglecting leakage fluxes, and ignoring the harmonics of flux density distribution in the air-gap.

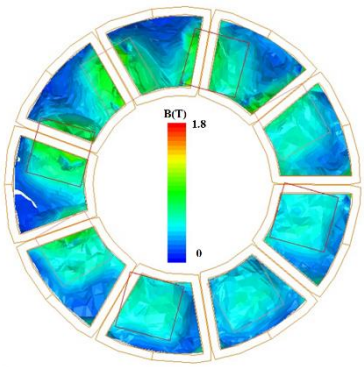

(a)

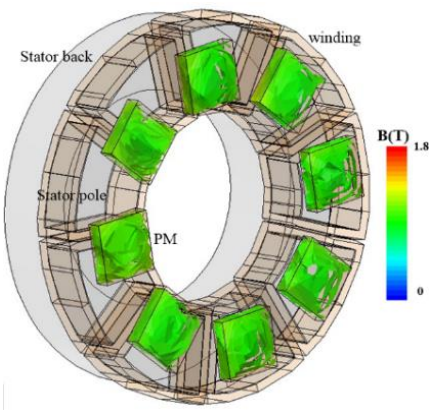

(b)

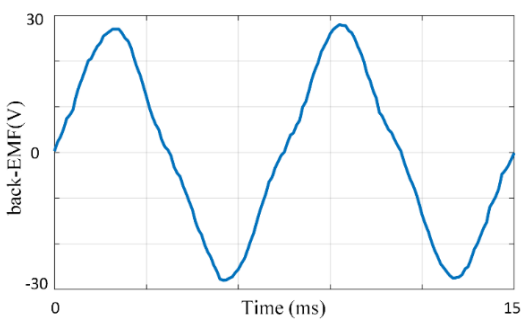

(c)

Fig. 4. Numerical results: a) magnetic flux density distribution in the 1st design generator poles, b) PMs, c) back-EMF

TABLE I
MAIN DESIGN SPECIFICATIONS, 2000 RPM, $p=4, s=9$

Parameter	Value	Parameter	Value
l_m	5mm	R_B	1 ohm
b_p	20mm	K_{loss}	0.05
$h_{s,\max}$	30mm	r_o	60mm
$B_{\max}$	1.7T	r_i	35mm
$A_{m,\max}$	20e3 A/m	g	1mm
$\eta_{\min}$	80%	B_{rm}	1.2
$P_{d,\min}$	150 watt	PM type	NdFeB35
E_B	24 V		

TABLE II
PARAMETERS OF THE DESIGNED GENERATORS

Parameter	#1	#2	#3	#4	#5
$h_s(mm)$	15	16	17	18	19
$h_{12}(mm)$	0	1	2	3	4
b_s/τ_s	0.2	0.2	0.2	0.2	0.2
$R_s(\Omega)$	0.229	0.229	0.229	0.229	0.229
$L_s(mH)$	0.533	0.568	0.604	0.639	0.674
N_s	78	78	78	78	78
$a_{Cu}(mm^2)$	0.785	0.785	0.785	0.785	0.785
Parameter	#6	#7	#8	#9	#10
$h_s(mm)$	20	21	15	16	17
$h_{12}(mm)$	5	6	0	1	2
b_s/τ_s	0.2	0.2	0.21	0.21	0.21
$R_s(\Omega)$	0.229	0.229	0.239	0.239	0.239
$L_s(mH)$	0.709	0.744	0.562	0.598	0.634
N_s	78	78	81	81	81
$a_{Cu}(mm^2)$	0.785	0.785	0.785	0.785	0.785

TABLE III
COMPARISON OF ANALYTICAL AND NUMERICAL RESULTS

Parameter	Numerical	Analytical
rms phase current	5.2A	5.9A
rms phase voltage	19V	20.6V
L_s	5.7mH	5.3mH
I_d	7.3A	7.6A
V_d	38.5V	39.2V
P_o	282watt	298watt

IV. PERFORMANCE EVALUATION OF DESIGNS

Now, for 10 resulted designs of previous sections, the main output characteristics are analyzed in this section. The variable

parameters for the operation range in question are the shaft speed and the duty ratio of the Cuk converter. The objective is to maximize power delivery to the battery at each speed.

Figs. 5 and 6 show the output characteristics that are the output power, the maximum power delivered to the battery, the generator efficiency, and the duty ratio for the defined objective. It should be noted that for other design objectives, different figures will be resulted.

Fig. 5 shows that the output and delivered power increase as the speed increases, but the rate of increase is different for different designs. Also, the working space is under the mesh as these figures show the boundaries.

Fig. 6a depicts that efficiency is directly related to the speed, and there is a large gap between the efficiency of designs 8-10 and the previous ones. As expected, the duty ratio in Fig. 6b decreases as the speed increases to regulate the output voltage of the converter.

Data in Fig. 6b could be used to control the converter so the maximum possible power delivery to the battery is achieved at different speeds.

These figures are dependent on the specifications of the battery. So, there exists a set of curves that show each output characteristic versus speed and battery specifications for a certain design.

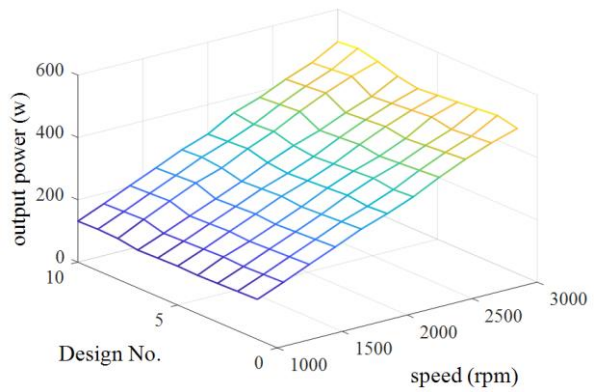

(a)

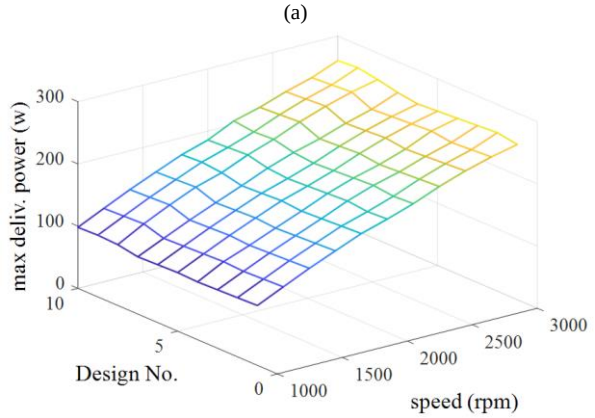

(b)

Fig. 5. The output characteristics of the valid designs: a) output power, b) power delivered to the battery

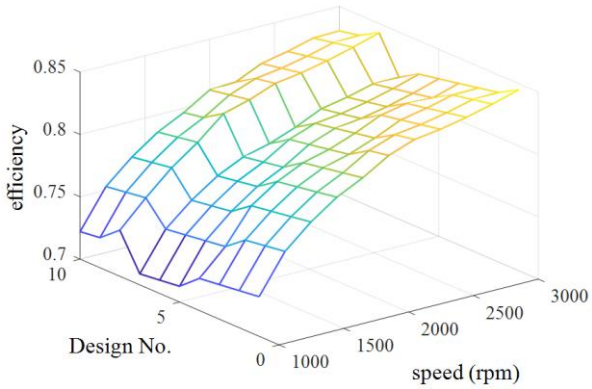

(a)

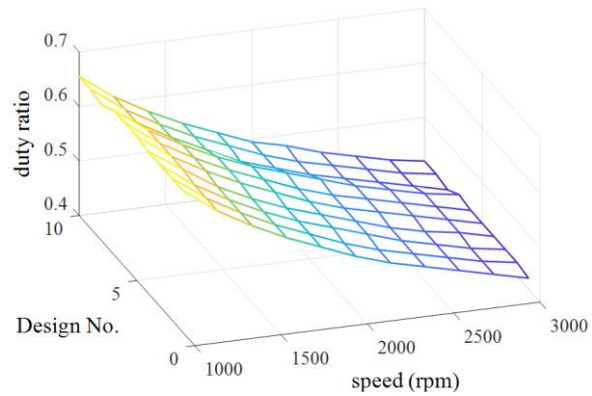

(b)

Fig. 6. The output characteristics of the valid designs: a) efficiency, b) duty ratio

V. CONCLUSIONS

This paper addresses the design and analysis of a portable power generation system. The key element of the system is the axial flux PM generator that has a considerable effect on the performance and output parameters of the system. The electrical model of the power generation system, design equations, constraints and approach for the generator design are presented. The design equations are validated by the finite element analysis and are used to design an AFPM generator for specific system requirements and parameters.

The presented method could be extended to other types of generators and could be utilized to design a similar fraction of horsepower portable power generation systems.

REFERENCES

[1] Yu-Shi Xue, Li Han, Hui Li and Li-dan Xie, "Int. Conference on Electrical Machines and Systems," *Optimal design and comparison of different PM synchronous generator systems for wind turbines*, pp. 2448–2453, 2008.

[2] M. Pinilla and S. Martinez, "Selection of Main Design Variables for Low-Speed Permanent Magnet Machines Devoted to Renewable Energy Conversion," *IEEE Trans. Energy Convers.*, vol. 26, no. 3, pp. 940-945, 2011.

[3] T. Yazdan, B. Kwon, "Electromagnetic design and performance analysis of a two-phase AFPM BLDC motor for the only-pull drive technique," *IET Electric Power Applications*, vol. 12, no. 7, pp. 999 – 1005, 2018
[4] Ji-Young Lee, Dae-Hyun Koo, Seung-Ryul Moon, Choong-Kyu Han, "Design of an Axial Flux Permanent Magnet Generator for a Portable Hand Crank Generating System," *IEEE Trans. Magn.*, vol. 48, no. 11, pp. 2977 – 2980, 2012.
[5] M. Bash, S. Pekarek, S. Sudhoff, J. Whitmore, M. Frantzen, "2010 Power and Energy Conference At Illinois (PECI)," *A comparison of permanent magnet and wound rotor synchronous machines for portable power generation*, pp. 1-6, 2010.
[6] I. Boldea, *VARIABLE SPEED GENERATORS*, Taylor & Francis, 2006.
[7] H. Polinder, F. F. A. van der Pijl, G-J. de Vilder and P. J. Tavner, "Comparison of direct-drive and geared generator concepts for wind turbines," *IEEE Trans. Energy Convers*., vol. 25, no. 3, pp. 725-733, 2006.
[8] B. Deok-Je, S. Ani, H, Polinder, L. Ji-Young, M. SeungRyul and K. Dae-Hyun, "Int. Conference on Electrical Machines and Systems," *Design of portable axial flux permanent magnet machines for human power generation*, pp. 414 - 417, 2010.
[9] J. Gieras, R. Wang and M. Kamper, *Axial Flux Permanent Magnet Brushless Machines*, Springer, 2008.
[10] P. Hekmati, R. Yazdanpanah, M. Mirsalim, E. Ghaemi, "Radial-Flux Permanent-Magnet Limited-Angle Torque Motors," *IEEE Trans. Ind. Electron.*, vol. 64, no. 3, pp. 1884-1892, 2017.
[11] F. Ebadi, M. Mardaneh, A. Rahideh, N. Bianchi, "Analytical Energy-Based Approaches for Cogging Torque Calculation in Surface-Mounted PM Motors," *IEEE Trans. Magn.*, vol. 55, no. 5, 2019.
[12] M. A. Noroozi, J. S. Moghani, R. Yazdanpanah, "Int. Power Electronics, Drive Systems and Technologies Conference (PEDSTC2015)," *Passive-rotor disk-shaped transverse-flux permanent-magnet generator for small wind turbine application*, pp. 25-28, 2015.
[13] Z. Nasiri-Gheidari, M. Ghods, H. Oraee, "Performance Analysis of Permanent Magnet Vernier Generator under Mechanical Faults," *International Journal of Industrial Electronics, Control and Optimization* , vol. 1, no. 2, pp. 121-131, 2018.
[14] A. Di Gerlando, G. Foglia, M. F. Iacchetti and R. Perini, "Analysis and Test of Diode Rectifier Solutions in Grid-Connected Wind Energy Conversion Systems Employing Modular Permanent-Magnet Synchronous Generators," *IEEE Trans. Energy Convers*., vol. 59, no. 5, pp. 2135-2146, 2012.
[15] M. H. Rashid, *Power Electronics Handbook; Devices, Circuits, and Applications*, Academic Press, 2007.
[16] N. Mohan, T. Undeland and W. P. Robbins, *Power Electronics: Converters, Applications, and Design*, JOHN WILEY & SONS, 1995.
[17] J. Cros and P. Viarouge, "Synthesis of high performance PM motors with concentrated windings," *IEEE Trans. Energy Convers*., vol. 17, no. 2, pp. 248–253, 2002.
[18] F. Magnussen and C. Sadarangani, "IEEE Int. Electric Machines and Drives Conf.," *Winding factors and Joule losses of permanent magnet machines with concentrated windings*, vol. 1, pp. 333-339, 2003.
[19] H. Vansompel, P. Sergeant, L. Dupre and A. Van Den Bossche, "A Combined Wye-Delta Connection to Increase the Performance of Axial-Flux PM Machines With Concentrated Windings," *IEEE Trans. Energy Convers*., vol. 27, no. 2, pp. 403-410, 2012.
[20] G. De Donato, F. G. Capponi and F. Caricchi, "Fractional-Slot Concentrated-Winding Axial-Flux Permanent-Magnet Machine With Core-Wound Coils," *IEEE Trans. Ind. Appl*., vol. 48, no. 2, pp. 630-641, 2012.
[21] F. Meier, "Permanent-Magnet Synchronous Machines with Non-Overlapping Concentrated Windings for Low-Speed Direct-Drive Applications", Ph.D. dissertation, Royal Institute of Technology, 2008.
[22] R. Yazdanpanah, M. Mirsalim, "Hybrid Electromagnetic Brakes: Design and Performance Evaluation," *IEEE Trans. Energy Convers*.," vol. 30, no. 1, pp. 60-69, 2015.

Reza Yazdanpanah received his B.Sc. degree in electrical engineering from Shiraz University, Shiraz, Iran, in 2003, his M.Sc. degree in electrical engineering from the Isfahan University of Technology, Isfahan, Iran, in 2006, and his Ph.D. degree in electrical engineering from the Amirkabir University of Technology, Tehran, Iran, in 2014. He is currently working with the Department of Electrical Engineering, University of Larestan, Lar, Iran. His current research interests include design of electric machines, DSP-based nonlinear control and drives, and power electronics.

IECO

This page intentionally left blank.